

Origin of the Meissner Effect and Superconductivity

John P. Wallace

*Casting Analysis Corp.,
8379 Ursa Lane, Weyers Cave,
Virginia 24486 USA*

Michael J. Wallace

*Freeport-McMoRan,
Phoenix, AZ 85050 USA*

Superconductivity in most metals is due to the activity of longitudinal spin waves binding electrons into pairs in such a way that the Meissner effect is generated along with the angular momentum responses in static magnetic fields. The bulk of these spin waves appear to be sourced by nuclear spins on the lattice. Experimentally longitudinal spin waves are not difficult to detect at room temperature as they form Bose-Einstein condensates that have onset temperatures, $> 1000^{\circ}K$, for the low mass entities, less than $10^{-40}kg$. These large scale quantum structures on the order of 1 meter are ubiquitous in metals and will also exist in space with low density matter where the ambient static magnetic fields are weak and temperatures are low. These massive boson collections probably are the source of the gravitationally detected dark matter in space and these experiments provide a test bed to understand their properties.^a

CONTENTS

I. Introduction	1
II. A Simple Experiment	2
A. Difference in Earlier Ferrous Experiment	3
III. Experimental Details	4
IV. Masses and Velocities	4
V. Bose-Einstein Condensates	6
A. Acceleration	7
VI. Superconductivity	7
VII. Inertia of a Longitudinal Spin Wave	7
VIII. Quantum Scale	8
IX. Discussion	8
Acknowledgments	9
References	9

I. INTRODUCTION

Most metals possess active nuclear spins in addition to the spins of their conduction electrons. Only a few metals are devoid a nuclear spin population, see Table I and II. It is easy to experimentally monitor longitudinal spin waves at room temperature in iron due to a small population of active participating electronic spins because they efficiently form a coherent Bose-Einstein

condensation with long lifetimes (Wallace, 2009a) (Wallace, 2009b). These spin waves have a wide velocity range due to their small mass, unlike phonon that propagates at a single velocity. These properties make the longitudinal spin wave, \mathbf{S}_{lsw} ideal for coupling with conduction electron spin, \mathbf{S}_e via a magnetic interaction $\mathbf{S}_{lsw} \bullet \mathbf{S}_e < 0$ allowing pairs to form a boson that supports superconductivity.

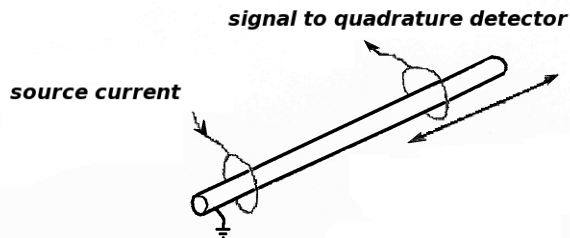
The recent announcements of near or above room temperature superconductivity in hydrogen rich alloys prompted a look at these spin rich alloys because of previous work where superconducting activity was found above $77^{\circ}K$ in foils of aluminum and niobium contaminated with hydrogen (Wallace, 2011). The question arose: Could longitudinal nuclear spin waves mediate electron pairing and superconductivity while explaining the Meissner effect? The answer turns out to be yes. Longitudinal spin waves seem to be ubiquitous in most metals. They have some important properties including a small mass which gives them a range of velocities much greater than the speed of sound. A question as why these spin waves have been missing in action for so long has a simple answer: No one bothered to look for them. This in part was due to the success of the Debye theory of heat capacity which had the phonon doing an impossible service that was not challenged.

Superconductivity is a completely non-classical phenomenon, poorly treated by modelers using a variation of quantum electrodynamics whose foundations are weak (Wallace and Wallace, 2023). Jorge Hirsch has logged a number of unanswered question about the inadequacy of the BCS model and later additions (Hirsch, 2009). The main complaint is about the inability of the modelers to explain the origin of Meissner effect. The phonon bond-

^a Version 3, 13 March 2024, viXra:2402.0017

ing hypothesis to create paired electrons is weak because longitudinal phonons operate at a fix velocity and possess no innate attractive potential, while electrons needing to be bound can be moving at considerably greater velocities. The BCS arguments also ignored the fact that T_c need not be isotope mass dependent via the phonon, as the band structure at low temperatures is extremely sensitive to isotope concentration ratios affecting the lattice parameter. The lattice parameter affects the band structure that plays a major role in fixing T_c .

Figure 1 *Source and detector arrangement for generating and detecting the fields and exciton in metals. The source is set near the end of the sample with a ground connection made to the bar close to the inductor to short circuit capacitive coupling to the bar. This is important because the nuclear longitudinal spin waves produce a reduced response of what is found in annealed iron.*



II. A SIMPLE EXPERIMENT

To show the existence of longitudinal spin waves requires only an induction source, a short coil, surrounding a long metal conductor. Very similar to the arrangement used in making eddy current measurements for properties or defects in metals (Wallace, 1987) (Wallace *et al.*, 1991) (Wallace, 2009a) (Wallace, 2011). However, instead of looking for the local eddy current response signal the detecting short coil is displaced away from the source to detect any propagating signals. The signal source and detector used was an SR865A lock-in-amplifier that allows an accurate measure of the amplitude and phase shift of a field created by its internal oscillator after traveling to a displaced detector coil. The instrument was operated over a frequency range of 1 kHz to 4 MHz in this geometry testing a number of different non-ferromagnetic metals.

The electromagnetic analysis of the eddy current boundary value problem induces a local current that opposes the applied AC field (Dodd and Deeds, 1968). The geometry of the rod will seem to restrict any propagating field to have an axial symmetry. In practice what is detected away from the source propagating down the bar is a portion of a spherical wave front that rolls off as $\sim 1/r^3$. This is because the solid angle the detector capture window goes as the *Sine* of the angle formed by

Table I **Some stable isotopes with nuclear magnetic moments for elements involved in superconductivity. The quantity P is used as a relative quality factor being the product of the % of isotopes in the metal with a nuclear magnetic moment's times the magnitude of their magnetic moment.**

$P > 100$	$P < 100$	T_c K°	Nuclear Mag. Moment %	Nuclear Moment	Moment $\times \% = P$
Nb		9.5	100	6.13	613
Tc		7.77	100	5.66	566
	Pb	7.19	22	.58	12.7
V		5.38	100	5.14	514
Ta		4.48	100	2.34	234
	Hg	4.15	30	-.55, +.50	15
In		3.4	100	5.51	551
	Sn	3.7	16	1.04	16
Tl		2.39	100	1.62	162
Re		1.4	100	3.17	317
Al		1.14	100	3.64	364
Ga		1.09	100	~ 2.2	220
	Mo	.92	24	$\pm .91$	22
	Zn	.875	4	.87	3.5
	Os	.65	18	.65	11.7
	Cd	.56	12	.21	2.5
	Zr	.54	11	-1.3	14
	Ru	.51	29	-.69, -.28	15
	Ir	.14	100	.16	16
	Hf	.12	32	.655	21
	W	.012	14	.12	1.7

dividing the bars diameter to the displacement of the detector from the source. The energy pumped into the bar at the source ends up producing a spherical wave and not one constrained by the cylindrical geometry of the experiment. These spherically propagating fields are generated directly by the applied time dependent field as they do not have the phase dependence of the induced currents.

The geometry of this wave front being spherical is not a surprise as its a form generating the minimum dissipation due to not being able to generate eddy currents losses on its own. As this is an oscillating magnetic signal in time normal to the spherical wave front it is easy to show that $\nabla \times H = 0$ in this geometry. Therefore, the wave front generates no induced currents from Ampere's Law $-\partial \mathbf{B} / \partial t = 0$. With no induced currents there are no eddy current losses. The detector simply records the

Table II Some stable isotopes with nuclear magnetic moments for elements involved in alloys that are superconducting.

Elements in SC	Nuclear Mag. Moment %	Nuclear Mag. Moment	Moment \times % = P
Li	100	3.2	320
H	100	2.79	279
F	100	2.63	263
Cs	100	2.56	256
B	100	2.5	250
Cu	100	2.3	230
As	100	1.43	143
D	100	.86	86
N	100	.4	40
K	100	.39	39
Y	100	-.14	14

response of the leakage field. A second test for the spherical wave front formation is to embed a source in a plate (Wallace and Wallace, 2011a) and on a circle centered on the source is to embed coils tangent to the circle around the source to monitor the roll off as a function of the angle from the normal to the source field. The fields only falls off 50% for a sensor perpendicular to the source at 90° from the source and this is due to geometry of source interfering with the generated field. Unlike in free space doing this same test the field is not extinguished when the source and detector are oriented to 90° to each other. As a check, a test was done with coils embedded in a niobium plate both in line and perpendicular to source and the results showed the characteristics of spherical wave front being generated.

When solving the electromagnetic boundary value problem for induced currents there is no solution predicting traveling longitudinal fields with spherical symmetry. The simple constitutive relations used in Faraday-Maxwell in Equations 1 do not cover the quantum mechanical effects of how energy, especially in non-static modes is passed to the spins of the system (Pauli, 1973).

$$\begin{aligned} \mathbf{B} &= \mu\mathbf{H} \\ \mathbf{J} &= \sigma\mathbf{E} \end{aligned} \quad (1)$$

Metals with a fraction of their isotope possessing nuclear spins are more common than metals with no nuclear spins. However, the most common with a very small fraction of nuclear spins is iron, where iron-57 is the only stable isotope possessing a nuclear spin in a concentra-

Figure 2 $1/r^3$ roll off in signal showing very little dissipation in an aluminum extruded tube .0127 meters in diameter with a .0013 meter wall thickness. This is the roll off expected for a spherical wave where the sensor has a finite sampling length along the bar. The $1/r^2$ roll off for a spherical wave is modified by the finite sampling length of the coil that goes as the $\sin(\theta)$ where θ is the angle of from the center of the source coil to the middle of the detector coil on the outside diameter of the sample. This produces the additional factor of $1/r$. The weak attenuation is feature of a uniform wave front that induces no local currents.

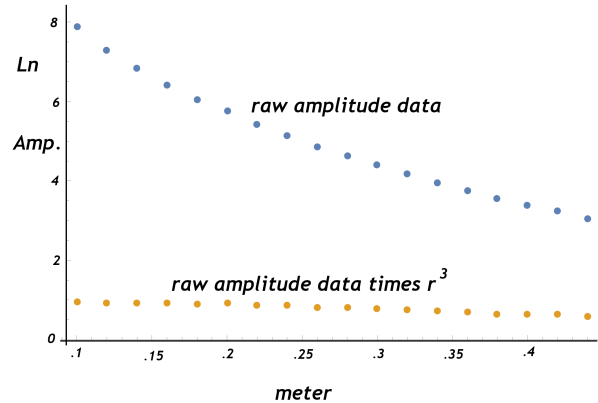
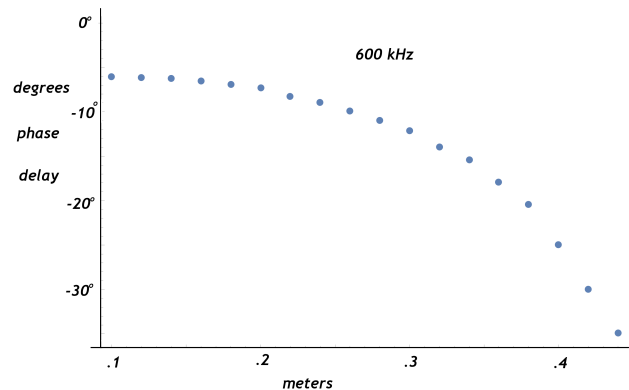


Figure 3 Phase data at 600 kHz where the error bars are less than the points size under .2 meters. There is an interesting feature about the phase data as the signal seems to be accelerating as it moves down the tube.



tion of 2.2%. This is fortunate since the electron spin concentration found in iron that are active in longitudinal spin waves can be compared to non-ferromagnetic metals where the nuclear spins should dominate the long range fields.

A. Difference in Earlier Ferrous Experiment

In the earlier experiments in well anneal iron it was possible at the highest measurement frequencies to show the density of the massive wave function peak away from

the origin at approximately .14 meters with no correction to the scaling of the data as a function of detector placement. Meaning, that by using the Compton relation for scale and mass, the mass of an individual exciton could be deduced by this measurement. The measurement is that of a coherent collection of individual excitons. Nominally, at rest the massive boson density function in its own self-reference frame peaks at $r = 0$, however, as the frequency is increased along with its velocity this amplitude at $r = 0$ drops and peaks at a displaced distance from $r = 0$. This is the behavior that under pins the CP violation for massive bosons, $W^\pm Z^0$, as the weak charge is no longer quantized. None of the other three particle families: massive fermion, and the massless boson and fermion show this behavior (Wallace and Wallace, 2014a). The non-ferrous longitudinal spin waves appear to be less massive and this peak would appear at a meter or more. With such a displacement the $1/r^3$ roll off would have the peak signal below the noise floor. The mass that can be measured now in these alloys is only that of the entire Bose-Einstein condensate of spin waves for non-ferrous metals.

One additional observation from the early work with iron is that if hydrogen is injected at the parts per million level into the iron then there are large, 20%, changes in transmission and phase shift changes that are abrupt. Normally these transmitted fields are immune to physical defects and large transverse magnetic fields, the only perturbation found to affect these transmission was interstitial hydrogen (Wallace, 2009b).

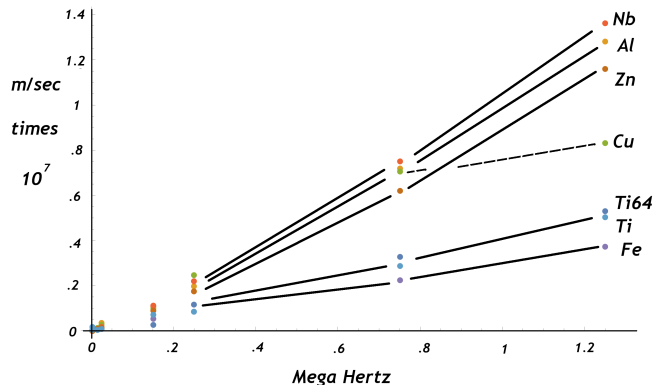
III. EXPERIMENTAL DETAILS

The experiment simply requires recording the amplitude in nanovolts and the phase angle in degrees after manually displacing a snugly fitted coil from the source at different positions on different metallic samples. While taking measurements at three different frequencies at each position so that the first and second derivatives, $\partial\omega/\partial k$ and $\partial^2\omega/\partial k^2$ can be numerically computed.

The sensor were made of 4 turns of #20 copper magnet wire with the detector having a series 50 ohm resistor. Very close to the source coil the bar was grounded with a woven copper strap to short circuit capacitive coupling between the coil and the bar. The source was driven at an amplitude of 2 volts which translates to a current range about 50 milliamps producing a field $\sim 10^{-5}$ Tesla at the center of coil with a diameter of .127 meters. Phase calibration is done with the source and detector coils empty but in the same orientation as the test. Those phase offsets are due to the circuitry and need to be subtracted from the measured data on a sample.

The current drive was at a lower level compared to the earlier work in iron where the drive level supported three simultaneous frequency just below an operating point

Figure 4 **Experimental data taken from 1 kHz to 1.5 Mhz on various metals detecting longitudinal spin waves. The phase delay data was taken at a fixed distance of .1 meters between the source coil and the detecting coil and was processed by equation 10 using three sampled frequencies 1-2-3 kHz, 100-200-300 kHz, and .5-1.0-1.5 MHz readings. The first observation is that these velocities easily exceed the speed of sound and seem to be ubiquitous regardless of the metal. We have found no metal example where these spin waves were not detect.**



where there was no non-linear behavior. The response in iron is significantly greater at the same drive levels, particularly at frequencies below 100kHz. Non-linear meaning where product states of the type $\omega_1 \pm \omega_2$ and $\omega_1 \pm 2\omega_2$ were produced. What is now being measured are not single exciton properties but the entire Bose-Einstein condensate made of a collection of components. Because of the low mass of the spin waves the BEC onset temperature is well above room temperature (Wallace, 2009a).

In both the ferrous and non-ferrous metals a strong transverse magnetic field of greater than .15 Tesla produces no effect on the spin wave propagation to the limits of the measurement. Whereas, the accuracy of the amplitude measurements can be made to within 1 or 2 nano volts the phase angle measurements are not as accurate because of the accumulated errors of the two quadrature channels especially at distances greater than .3 meters. At .1 meters and under it is possible to measure the absolute phase angles to .01° degrees of arc.

IV. MASSES AND VELOCITIES

Generating a relativistic dispersion curve cannot be done by applying $\gamma = 1/\sqrt{1-v^2/c^2}$ to the non-relativistic relation that comes out of the Schrödinger equation.

$$E = \gamma \frac{\hbar^2 \kappa^2}{2m} \quad (2)$$

This fix is a patch that does not correct the underlying problem that the Schrödinger equation is non-relativistic. One cannot use the Dirac equation as it has two major defects. The first fault is being a forced linear expression that ignores the quadratic nature of the relativistic conservation of energy relation $E^2 = p^2c^2 + (mc^2)^2$ and secondly it uses Oskar Klein's energy operator that is non-relativistic as it dropped the constant self-energy mc^2 . The same defect holds true for the Klein-Gordon equation even though it starts out with the correct expression. To generate the correct dispersion relation the complete relativistic wave equation (Wallace and Wallace, 2023) in the laboratory frame will be used for the longitudinal spin wave that has two additional terms compared to the Schrödinger equation:

$$\frac{\hbar^2}{2m} \left\{ \nabla^2 \phi - \frac{1}{c^2} \frac{\partial^2 \phi}{\partial t^2} \right\} + i\hbar \frac{\partial \phi}{\partial t} = \left(V + \frac{V^2}{2mc^2} \right) \phi \quad (3)$$

With the potential being zero, $V = 0$, the equation reduces to:

$$\frac{\hbar^2}{2m} \left\{ \nabla^2 \phi - \frac{1}{c^2} \frac{\partial^2 \phi}{\partial t^2} \right\} + \frac{2im}{\hbar} \frac{\partial \phi}{\partial t} = 0 \quad (4)$$

The trial solution for a spherical wave is:

$$\phi(r) = A \frac{e^{i(\kappa r - \omega t)}}{r} \quad (5)$$

This yields the dispersion relation on substituting equation 5 into 4:

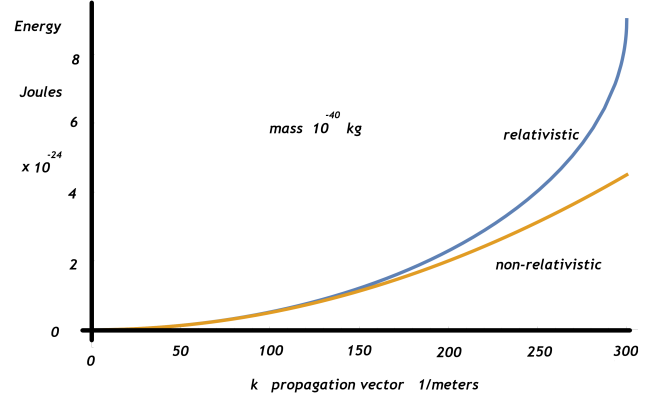
$$\begin{aligned} \omega^2 - \frac{2mc^2}{\hbar} \omega + c^2 \kappa^2 &= 0 \\ E = \hbar \omega &= mc^2 \left\{ 1 - \sqrt{1 - \frac{\hbar^2 \kappa^2}{m^2 c^2}} \right\} \end{aligned} \quad (6)$$

From the raw phase shift data at a fixed displacement along the bar or plate as function of frequency it is possible to estimate the spin wave velocity and its mass by taking the first and second derivatives. The propagation vector, κ , is determined by the measured phase shift of the field, θ as a function of displacement, r .

$$\kappa(\omega) = \frac{\theta(\omega)}{r} \quad (7)$$

Both r and θ can be measured so that k can be computed. Numerically both the first and second derivative of $\omega(\kappa)$ as a function can be estimate when $\omega_2 - \omega_1 = \omega_1 - \omega_0 = \Delta\omega$. In order to compute both the velocity and mass of the longitudinal spin waves two numerical derivatives are required

Figure 5 The relativistic dispersion curve from equation 6 is compared to the non-relativistic form $E = \hbar^2 \kappa^2 / 2m$ that is a simple parabola.



$$\frac{\Delta\omega}{\Delta\kappa} = \frac{r\Delta\omega}{\theta_1 - \theta_0} \quad (8)$$

$$\frac{\Delta^2\omega}{\Delta\kappa^2} = 2\Delta\omega \frac{2\theta_1 - \theta_2 - \theta_0}{(\theta_2 - \theta_0)(\theta_2 - \theta_1)(\theta_1 - \theta_0)} r^2$$

Taking the derivative of ω with respect to the propagation vector, κ , in equation 6 is the first step.

$$\frac{\partial\omega}{\partial\kappa} = \frac{v}{\sqrt{1 - \frac{v^2}{c^2}}} \quad (9)$$

$$v = \frac{\partial\omega}{\partial\kappa} \frac{1}{\sqrt{1 + \frac{\partial\omega^2}{\partial\kappa^2}}} = \frac{\Delta\omega}{\Delta\kappa} \frac{1}{\sqrt{1 + \frac{\Delta\omega^2}{c^2}}} \quad (10)$$

In order to extract the mass, m , a relation using the second derivative of equation 6 of ω with respect to the propagation vector is required, where $\gamma = 1/\sqrt{1 - v^2/c^2}$.

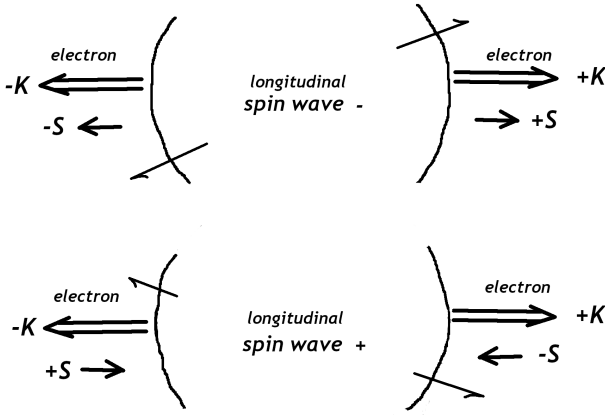
$$\frac{\partial\omega}{\partial\kappa} = \frac{\hbar}{m} \frac{\kappa}{\sqrt{1 - \frac{\hbar^2 \kappa^2}{m^2 c^2}}} \quad (11)$$

$$\frac{\partial^2\omega}{\partial\kappa^2} = \frac{\hbar}{m} \gamma \left\{ 1 + \frac{v^2}{c^2} \gamma^2 \right\} \quad (12)$$

$$m = \frac{\hbar}{\frac{\Delta^2\omega}{\Delta\kappa^2}} \left\{ \gamma + \frac{v^2}{c^2} \gamma^3 \right\} \quad (13)$$

Now the velocity and the mass can be computed from the data. These are not single particle velocities rather the velocity and mass of Bose-Einstein condensation as a whole.

Figure 6 *Longitudinal spin wave's spherical propagating wave front is a large scale structure with a long wavelength on the order of a meter compared to a scale required to bind electrons. A single spin wave has the capacity to bind opposite momentum electrons to produce a zero momentum state for the bound pair. The pair can then interact with an external field so long as the field does have the strength to break the magnetic bond between the propagating spherical wave front of the longitudinal spin wave and the electron's spin. What is required of the spin wave is a velocity that matches the electrons' velocities. Because the longitudinal spin waves being a spin 0 boson possess mass they have a range of velocities from zero upwards unlike the phonon that only operates at the speed of sound.*



V. BOSE-EINSTEIN CONDENSATES

A strong transverse magnetic field had no measurable effect on the transmission of the signals, however, a small longitudinal static magnetic field at the source coil $\sim 2.5 \cdot 10^{-5}$ tesla had a measurable effect of reducing the signal by $7.85\% \pm .2\%$ that was found to be almost independent of the material under test, see Table IV.

The prime interaction of the static longitudinal magnetic field main effect will be with the strongest moment. The strongest moment will be the axial moment of the longitudinal spin wave. Because of this interaction it is possible to get a measure of the bound state energy forming the spin wave by using the ratio of the Boltzmann statistic between measurements with and without the applied static field.

Table III The Fe samples were taken at 80-120-160 kHz all the others were taken at .5-1.0-1.5 MHz. Al tube and Cu, Ti64, Fe rods were .127 m in diameter except for the W rod that was .0095 m in diameter. The pure Nb and Ti samples ($< 99.9999\%$ metal purity however these bars probably contain a significant amount of hydrogen) had rectangular cross sections of $.0034 \times .0112$ m and $.0051 \times .0117$ m respectively. The copper sample was annealed oxygen free high conductivity. The iron was 99.9% metal content and the aluminum, zinc, and Ti64 were commercial grade.

metal	Velocity range $\times 10^6 m/sec$	Mass .5 - 1 - 1.5 MHz $\times 10^{-37} kg$
Fe	.031 - 3.7	16.7
Nb	.07 - 12.8	1.31
Al	.041 - 13.5	1.14
Ti64	.016 - 5.0	8.65
Ti	.03 - 5.3	8.31
Zn	.0075 - 11.6	1.56
W .12 m	7.6 - 17.2	.68
Cu	.01 - 1.5	6.88

$$\frac{n_1}{n_o} = e^{-\frac{E}{kT}} = \frac{1}{1.0785} = .9272$$

$$Ln \frac{n_1}{n_o} = -\frac{E}{kT} = -.07551 \quad (14)$$

$$E = 1.906 \times 10^{-3} eV$$

Since we know the value of the applied static longitudinal field the energy can be computed.

$$E = \mu \bullet \mathbf{B} = 1.906 \times 10^{-3} eV \quad (15)$$

$$\mu \sim 1.23 \times 10^{-17} J/t$$

This magnetic moment is much greater than an electron or a nucleus. It is the magnetic moment of an entire Bose-Einstein condensate that forms the longitudinal spin wave. There does not appear to be a simple way to

Table IV 1 Mhz readings for an axial static magnetic field effect on transmission. Similar results were found at 20 kHz. All samples were .0127 meters in diameter data taken over .1 meter. There was no measurable phase change with or without the static longitudinal B field. The static B field was driven by a DC current of 74 milliamps into the source coil results in a field of approximately 2.5×10^{-5} tesla estimated from the relation for a short solenoid and confirmed with a gauss meter.

Metal	$B = 0$ Amp. $nV \pm 1 nV$	$B \sim 2.5 \cdot 10^{-5}$ tesla Amp. $nV \pm 1 nV$	ratio
Cu	3,771	3,492	1.0798
Zn	3,487	3,234	1.078
Fe	11,754	10,908	1.0775
Ti64	4,393	4,065	1.0806
Al	3,999	3,714	1.0767

tell what spins are actually participating in this ensemble. It does give a count that is a large number between 10^6 and 10^9 spins. However, the spin density, n , over the volume covered by the source inductor ranges from 1.5×10^{13} to 10^{16} n/m^3

$$T_{BEC} = \frac{2\pi\hbar^2}{mk} \left\{ \frac{n}{\zeta(\frac{3}{2})} \right\}^{\frac{2}{3}} = 3.3125 \frac{\hbar^2 n^{\frac{2}{3}}}{mk_b} > 1000^\circ K \quad (16)$$

Taking the mass of the electron longitudinal spin wave in iron at 10^{-40} kg and for the nuclear spin waves at one to two orders of magnitude less at 10^{-41} to 10^{-42} kg. The transitions temperature in all cases is well above $1000^\circ K$.

The signature of this independent quantum entity is the fact that the loss ratio over the five very different metals and alloys in Table IV is the same. This independence from the substrate on which the Bose-Einstein condensation forms is the characteristic a quantum encapsulation of properties that can take place when the massive bosons are forced to be in their ground state. The Bose-Einstein condensation can then be treated as a whole when doing mechanics. There is another feature of this state that should be noted and that is the BEC state offers some stability to the individual spin waves which have a finite lifetime. The analogous situation is the stability of neutrons within stable isotopes.

A. Acceleration

In Figure II there is a noticeable increasing phase delay at the larger distances. It appears the Bose-Einstein

condensate is accelerating. That can be confirmed by computing the velocities and mass as the distance from the source increases. So that experiment was repeated and .1, .15, and .2 meters data was taken to compute the mean velocity and mass in Table V.

Table V Acceleration of a Bose-Einstein condensation in a .0127 diameter aluminum tube with a wall thickness of .0013meters. Data taken at .5, 1, and 1.5 MHz by measuring the phase offset from the source.

Distance meters	Mean Velocity $\times 10^6 m/sec$	Mass $\times 10^{-38} kg$
.1	9.4	16
.15	13.6	7
.2	17.8	3

As the BEC moves down the tube it will shed some its strength radially and that is what is measured. However, the spin wave's motion is axially down the tube and this lost field represents lost mass of the Bose-Einstein condensate. In order to conserve momentum from the lost mass the velocity of the Bose-Einstein condensate will increase. That is exactly what has been detected. This is another proof that the signals detected are from a Bose-Einstein condensation. As this is a tube, field will be lost from two surfaces and the effect is enhanced.

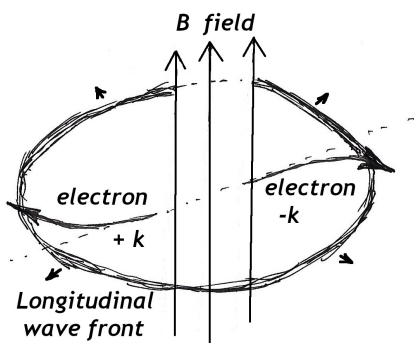
VI. SUPERCONDUCTIVITY

The shielding of the electrons that participate in forming pairs to act as a boson in a superconductor is an essential feature for a metal becoming superconducting. Hirsch noted only hole conductors have superconducting properties. He was concerned about charge imbalances going through the superconducting transition. The imbalances would be caused by the effect of a free surface on particle motion. Only a more agile hole charge carrier could screen the superconducting interior from stray fields. Any long range electrostatic field at that point would inhibit the transition to superconductivity. The facility of having a spin free screening agent, holes, more agile than the electrons is a major feature of the entire process.

VII. INERTIA OF A LONGITUDINAL SPIN WAVE

The principal inertia the spin wave must overcome is the inertia due to rotating its magnetic moments. In iron the inertia of a free electron is about two orders of

Figure 7 In order to achieve the Messiner effect there are three important details. First a longitudinal spin wave must couple two electrons via their spins. The two electrons will have opposing spins aligned along their direction of motion. The second requirement is those two electrons have opposite propagation vectors, κ . The third requirement is the presence of a perpendicular magnetic field to the propagation vectors forcing the electrons to rotate without breaking their connection to the longitudinal spin wave. This rotation about the B-field will cause the imposed external field to be canceled producing the Meissner effect. These rotating electron pairs will now have an axial angular momentum and for angular momentum to be conserved the solid they are in will rotate in the opposite direction.



magnitude greater than that for the nuclear spins, see Table VI. This correlates to the velocity difference between the two groups. The interesting entity is the proton, that is extremely supple and may contribute to its alloying efficiency in superconductors.

VIII. QUANTUM SCALE

The question of quantum mechanics being limited to the atomic scale or smaller no longer carries any validity as we are dealing quantum structures on the order of a meter, with very small masses for entities that can exist in regions of matter or in low density space if the local magnetic fields are sufficiently weak.

Mass can be carried by massive fermions and massive bosons. In this case an exciton that is a massive spin 0 boson has mass in a metal if the static \mathbf{B} -field is weak or nonexistent so the spins are free to support longitudinal spin waves. In regions of space where there is low density matter and weak magnetic fields these spin waves can exist both with large physical scales and in great numbers.

Table VI Moment of inertia estimated using the charge radius and the mass in the relation $mr^2/2$. For the free electron the electrostatic charge radius was used (Wallace and Wallace, 2015). For the nucleons the relation $1.25 \times A^{1/3} fm$ was used where A is the mass number. The free electron behavior might be reflected in the spin wave behavior in iron. Where the other non-ferrous metals have a reduced over rotational inertia by two orders of magnitude.

isotope	mass kg $\times 10^{-27}$	radius meters $\times 10^{-15}$	I $\times 10^{-60}$ $m kg^2$	I $\times \mu$
bound ele.	.00091	$\sim 1 \ 10^5$	$4.55 \ 10^{-51}$	$4.22 \ 10^{-74}$
free ele.	.00091	$7.72 \ 10^2$	$2.71 \ 10^{-55}$	$2.52 \ 10^{-78}$
^{201}Hg	336.378	7.18	$8.67 \ 10^{-54}$	$2.42 \ 10^{-80}$
^{199}Hg	333.027	7.18	$8.58 \ 10^{-54}$	$2.16 \ 10^{-80}$
^{93}Nb	155.5038	5.578	$2.42 \ 10^{-54}$	$7.51 \ 10^{-80}$
^{27}Al	45.160	3.71	$3.10 \ 10^{-55}$	$5.7 \ 10^{-81}$
proton	1.67262	.87	$6.33 \ 10^{-60}$	$8.928 \ 10^{-86}$

IX. DISCUSSION

Superconductivity was discovered in 1911, however, in 1912 Peter Debye proposed a seemingly successful theory from statistical mechanics to explain solid state heat capacity (Eisberg and Resnick, 1985). Planck used as the basis of his model for black body radiation a cavity that was filled with photons. Debye used the same model but replaced the photons with phonons, lattice vibrations. The problem with this replacement was the selected frequency range from zero to 10^{12} hertz for Debye's lattice vibrations. Debye did not know that above 10^8 hertz these lattice vibrations are strongly attenuated and break down into supporting local vibrational modes and are no longer long range travelers (Bhatia, 1967). The question is why did Debye's model that requires the long range movement of boson fields succeed? What was taking the place of the lattice vibrations? Could the longitudinal spin waves be the replacement for the missing high frequency phonons?

To support large scale quantum structures in space like the energy bubbles and dark matter requires a very low mass entity like the longitudinal spin wave (Wallace and Wallace, 2011b) as the basic building block. When solv-

ing the relativistic state equation in the frame of reference of the particle/field (Wallace and Wallace, 2014a) there are very few solutions out of the four different groups of particle – massive and massless fermions and bosons. The massive particles are characterized by being longitudinal fields. The only solution that allows the formation of Bose-Einstein condensation are the massive bosons. The only elementary massive boson is the $W^\pm Z^0$ particle that is unstable and extremely compact because of its enormous self-energy. At the other end of the scale are the longitudinal spin waves operating on matter that can exist over an extreme range of scales, densities, and lifetimes. These collections of spin waves can act as a sink and source of low energy fields. The low temperatures found in space will promote the formation of longitudinal Bose-Einstein condensates when excited by passing **B**-field transients. These spin waves will become a reservoir of mass in regions distant from the emissions of hot stellar cores.

One of the key details that came out in this study is the central role of the spherical wave front as the solution for the BEC. It is also the general solution for a photon and its importance is that as a propagating front encompassing all the mass it passes leading to the gravitational red shift (Wallace and J., 2021). Both areas of investigation into dark matter and dark energy have been hampered by sloppy dealings with the basics of quantum mechanics. A great deal of effort has been wasted on searching things that do not exist and ignoring the properties of matter that does exist.

ACKNOWLEDGMENTS

The authors want to thank Sampath Purushothaman who brought up the matter of hydrogen alloyed metallic high temperature superconductors.

Data Availability

The data that support the finding of this study are available from the corresponding author upon reasonable request.

Conflict of Interest

The authors have no conflict of interest to disclose.

REFERENCES

- Bhatia, A. B. (1967), *Ultrasonic Absorption* (Oxford Press, Oxford).
- Dodd, C., and W. E. Deeds (1968), *J. App. Phys.* **39**, 2829.
- Eisberg, R., and R. Resnick (1985), *Quantum Physics of atoms, molecules, solids, nuclei, and particles*, 2nd ed. (John Wiley and Son, NYC).
- Hirsch, J. E. (2009), “Bcs theory of superconductivity: the worlds largest madoff scheme?,” arxiv 0901.4099.”
- Pauli, W. (1973), *Pauli Lectures on physics volume 1 Electrodynamics* (MIT Press, Cambridge).
- Wallace, J. (1987), “us patent 4,651,094.”
- Wallace, J. (2009a), “Electrodynamics in iron and steel, arxiv:0901.1631v2 [physics.gen-ph],”.
- Wallace, J. (2009b), *JOM* **61** (6), 67.
- Wallace, J. (2011), in *SSTIN10 AIP Conference Proceedings 1352*, edited by G. Myneni and et. al. (AIP, Melville, NY) pp. 205–312.
- Wallace, J., and W. M. J. (2021), *Infinite Energy* **157**, 18.
- Wallace, J., J. K. Tien, J. Stefani, and K. Choe (1991), *J. of Applied Physics* **69**, 550.
- Wallace, J., and M. Wallace (2011a), *Dark Matter from Light extending quantum mechanics to Newton’s First Law* (Casting Analysis Corp., Weyers Cave, VA).
- Wallace, J., and M. Wallace (2014a), *The Principles of Matter amending quantum mechanics* (Casting Analysis Corp., Weyers Cave, VA).
- Wallace, J., and M. Wallace (2014b), viXra:1405.0015v1.
- Wallace, J., and M. Wallace (2015), in *Science and Technology of Ingot Niobium for Superconducting Radio Frequency Applications*, Vol. 1687, edited by G. Myneni (AIP, Melville, NY) pp. 040004–1–14, *Electrostatics*.
- Wallace, J., and M. Wallace (2023), *J. Phys. Astro.* **11** (4), 337.
- Wallace, J., and M. J. Wallace (2011b), in *SSTIN10 AIP Conference Proceedings 1352*, edited by G. Myneni and et. al. (AIP, Melville, NY) pp. 313–335.